GEOPHYSICAL RESEARCH LETTERS, VOL. ???, XXXX, DOI:10.1029/,

Multi-point observations of the inner boundary of the plasma sheet during a substorm

A. Runov,[1] V. Angelopoulos,[1] N. Ganushkina,[2] R. Nakamura,[3] J. McFadden,[4] D. Larson,[4] I. Dandouras,[5] K.-H. Glassmeier,[6] C. Carr[7]

A. Runov, Institute of Geophysics and Planetary Physics, University of California, Los Angeles, 3845 Slichter Hall, Los Angeles, CA-90095, USA. (arunov@igpp.ucla.edu)

[1]Institute of Geophysics and Planetary Physics, University of California, Los Angeles, CA-9095, USA

[2]Finnish Meteorological Institute, 11010 Helsinki, Finland

[3]Space Research Institute, Austrian Academy of Sciences, Graz, Austria

[4]Space Science Laboratory, University of California, Berkeley, CA, USA

[5]CESR/CNRS, Toulouse, France

[6]Institut für Geophysik und Extraterrestrische Physik, Technische Universität Braunschweig, Germany

We report on the THEMIS and Double Star TC-1 observations at the geocentric distances 3< R <8 R_E during a substorm on March 23, 2007. THEMIS crossed the equatorial dusk-side plasma sheet and inner magnetosphere in the pearls-on-string configuration, allowing to trace the dynamics of particle populations within time ranges from hours to 10 minutes. Data analysis shows co-existence of the plasma sheet ion population (5 - 30 keV) with the ring current ion population (100 - 1000 keV) at the geocentric distances 4 - 6 R_E. The plasma sheet population was characterized by pronounced "nose"-like dispersion with the spectral density maximum at ∼10 keV. The plasma sheet boundary, defined by a sharp decrease of the ∼1keV electron flux, moved inward to R=4 and outward back to ∼8 RE within about 1 hour. Local enhancements of the plasma sheet (1 - 5 keV) electron flux with the characteristic time scale of 2 - 10 min were detected at the geocentric distances between 5 and 6 R_E during the substorm.

[7]The Blackett Laboratory, Imperial College London SW7 2BW, UK

1. Introduction

The magnetotail plasma sheet (PS), containing high-β plasma with the typical ion energy of 5 - first tens of keV and electron energy 1 - 5 keV, is an important source of the hot plasma, observed in the inner magnetosphere. The inner edge of the PS is located at X ~-8 - -10 R_E at midnight during quiet time. During active time, PS particles have temporally limited access to the innermost regions of the magnetosphere [e.g., *Ganushkina et al.*, 2000; *Friedel et al.*, 2001; *Wang et al.*, 2004]. Existing models are able to reproduce PS particles entry to the inner magnetosphere (L <8) in the time range of several -10s hours, i.e., in the time range of magnetic storms. The models including quasi-static global electric field well reproduce observable feature such as ion "nose"-like dispersion, ion and electron convection boundaries [*Ejiri et al.*, 1980; *Kerns et al.*, 1994; *Angelopoulos et al.*, 2002]. On the other hand, it was found that closest to the Earth ion population, forming a nose-like structure, may move from geostationary orbit into the plasmasphere up to L=4.7 in about 1 hour during a substorm [*Ganushkina et al.*, 2001]. Local electric and magnetic fields varying in a time range of several - 10s min are indispensable to models [*Sergeev et al.*, 1998]. It has been shown that the inward displacement of the intense nose structure can occur under short-lived pulse electric fields [*Li et al.*, 1998]. Large-scale convection alone leads to the nose structure formation, which takes more than 5 hours [*Buzulukova et al.*, 2003]. The implication of more adequate global electric field models [e.g., *Angelopoulos et al.*, 2002] does not reduce this time sufficiently.

Multi-point observations of the dynamics of the inner PS are required to separate effects of the global convective and the transient electric fields. Four Cluster spacecraft provided valuable observations at high latitudes [e.g., *Apatenkov et al.*, 2007] and at $4\,R_E$ at all LT range on the equator [*Vallat et al.*, 2007] and simultaneously in opposite MLT sectors in correlation with the Double Star TC-1 spacecraft [*Dandouras et al.*, 2008]. The THEMIS mission provides an opportunity to probe the near-equatorial magnetosphere at a wide range of the geocentric distances [*Angelopoulos*, 2008]. At the initial phase, five THEMIS probes scan the dusk sector of the equatorial magnetosphere in a string-of-pearls configuration (apogee at 14.7 R_E), crossing geostationary orbit with time lags of 3 hours and of 10 minutes, enabling to resolve dynamics of the inner boundary of PS during substorms.

In this letter we report on multi-point probing of ion and electron population [dynamics of the electron population was not studied by *Ganushkina et al.*, 2001] in the transition region between the dusk-side PS and the inner magnetosphere during enhanced geomagnetic activity. The aim of this study is to reveal the temporal evolution of the inner edge of the plasma sheet on substorm time scales in order to determine the physics necessary to explain or properly model its behavior.

2. Data

We discuss THEMIS and Double Star TC-1 observations during a unique event on March 23, 2007. During the interval of interest, 11 - 20 UT, IMF B_z, according to ACE and WIND observations, experienced repeating north-south turns. The K_p index varied form 0+ to 3+. The AL index was less than -150 nT with two major peaks of -300 and -700 nT between 11 and 19 UT. THEMIS in-situ observations in the dusk-side plasma sheet as well as the ground-based observations during this event are intensively studied [*Angelopoulos et al.*, 2008, and papers in this issue].

Figure 1 shows the pseudo-AE index, calculated from the THEMIS ground based magnetometers and the potential difference across the polar cap ($\nabla\Phi$), calculated from the SuperDARN data, for March 23, 2007. In agreement with the provisional AL index from the Kyoto monitor, THEMIS pseudo-AE (further AE) shows enhanced activity with two peaks between 11 and 19 UT. The five THEMIS probes were at the same orbit with apogee at 14.7 R_E. During the inbound motion, they crossed the inner edge of PS at LT≈23:10 with UT lags of 3 hours (between THC and THD), 10 min (between THD and THB, and THB and THA), and 2.5 hours (between THA and THE). TC-1 was in the dusk-side PS, crossing its inner edge simultaneously with the THDBA-cluster at LT≈20:00 (Figure 1, bottom panel). THC crosses the inner edge of PS again at LT≈16:30 during its outbound motion. All SC probed the PS inner edge during enhanced magnetospheric activity with AE varying between 100 and 700 nT, and $\nabla\Phi$ scattering in a wide range between 45 and 70 mV (Figure 1, upper panels).

Figure 2 presents ER spectrograms of ions with energies of 1 - 1000 keV and electrons with energies 0.1 - 25 keV, obtained by the THEMIS ESA [*McFadden et al.*, 2008] and SST [*Larson et al.*, 2008] instruments during inbound crossings of radial distances of 3 - 8 R_E at LT≈23:10. The differential energy flux (DEF) exceeding the thresholds of 10^5 and 10^6 eV/(cm^2 s sr eV) for SST and ESA ions, respectively, and 10^7 for electrons is color-coded. The white space corresponds to the flux below the threshold. Penetrating radiation results in a background flux in the ESA detector with uniform counts background [*McFadden et al.*, 2008]. This was removed from the spectra by background subtraction.

Figure 3 shows the ion ER spectrogram obtained by TC-1 HIA instrument [*Rème et al.*, 2005] and ion and electron ER spectrograms collected by THC (outbound crossing) within distances of 3 - 8 R_E at 20:00 and 16:30 LT, respectively.

The leading probe (THC) passed the geocentric distances $8 > R > 3\,\mathrm{R}_E$ during 1112 - 1408 UT (interval I in Fig. 1). AE first increased up to 350 nT, then decreased down to 200 nT. The average potential difference across the polar cap $\langle\Delta\Phi\rangle$ increased from 50 to 65 mV. THC detected the decrease of the 5 - 10 keV electron flux at $8 > R > 7\,\mathrm{R}_E$ with a pronounced dispersion. The 0.5 - 5 keV electron flux, exceeding the threshold, was detected closer to the Earth, with a sharp cut off at $R \approx 5\,\mathrm{R}_E$. A depletion in the spectra, where $\sim$5 keV electrons were not present, was detected at $7 > R > 6\,\mathrm{R}_E$.

THD, THB, and THA, separated by $0.4\,\mathrm{R}_E$, crossed the region between R=8 and $3\,\mathrm{R}_E$ about 3 hours later, between 1350 and 1717 UT during the peak of AE and $\Delta\Phi$ varied between 55 and 80 mV with $\langle\Delta\Phi\rangle \approx$64 mV (interval II in Fig. 1). According to THD and THB observations, the $E >$5 keV electron boundary moved inward to $R \approx 6\,\mathrm{R}_E$. The boundary of the 0.5 - 5 keV electrons is detected at R=4.2 R_E: about 1.5 R_E closer to the Earth than it was observed by THC. The depletion in the electron spectra became deeper (down to $\approx$1 keV), and moved to $R \approx 6.5$ - 5 R_E. The electron spectrum, obtained in the same region by THA 10 minutes later, shows a reduction of the $E \sim$5 keV electron flux at $6 < R < 7\,\mathrm{R}_E$. The enhanced flux with a set of quasi-periodic maxima appears between $R \approx 6$ and 5.

THE, crossing the same region about 2.5 hours later than THA (interval III in Fig. 1), detected the boundary of the PS electron flux ($0.5 < E < 10$ keV) at R=7 R_E at 1800 UT.

THC, during its outbound motion, detected the electron PS boundary at R=8.3 R$_E$ at 18:30 UT.

The information on the location of the ∼1 and ∼5 keV electron boundaries (radial distances and local times), and the GSM magnetic field components from THEMIS/FGM [*Auster et al.*, 2008] at these points is summarized in Table 1.

The most distinctive feature in ion ER spectrograms is the presence of high phase space density population with energies between 5 and 50 keV, visible partly in SST and partly in ESA spectrograms. This ion population, characterized by pronounced nose-like dispersion with a spectral density maximum at E ∼10 keV, co-exists with the ions of 100 keV - 1 MeV ions, forming the outer radiation belt (ring current). This population was detected by THC between R=7.5 and 4.7 R$_E$. Three hours later, this population was detected by THD, THB, and THA between R ≈6.0 (6.4, THA) and 3.8 R$_E$. The trailing THEMIS probe, THE, passing 8> R >3 R$_E$ region 2.5 hours later than THA, detected the population of 5 - 20 keV ions with nose-like dispersion between R=6.5 and 4.5 R$_E$ with reduced flux density.

During 1529 - 1700 UT TC-1 crossed the sector of the equatorial PS between 18 and 20 LT at 6.5> R >3.5 R$_E$, detecting a distinct nose-like dispersion of the ion energy flux with the peak at 10 - 11 keV (Fig. 3, upper panel). THC crossed the region of geocentric distances 3< R <8 R$_E$ at ∼16 LT during 1614 - 1910 UT, i.e., roughly simultaneously with THE. The ion population with energies 10 - 40 keV was detected at 4.2< R <7.0 R$_E$ (Fig. 3). No enhanced flux of ions with energy <10 keV, detected at the same time by THE at 23 LT, was observed.

Table 2 summarizes the UT, coordinates (R and LT) of the observed ion nose-like structure, and the magnetic field from THEMIS and TC-1 [*Carr et al.*, 2005] FGM instruments at the nose locations.

Since neither inward-outward motion of the electron plasma sheet boundary, nor ion nose-like structures were observed on the previous THEMIS orbit, these signatures may be attributed to the substorm activity during 1100 - 1900 (see Fig. 1).

Figure 4 shows the electron energy-time (ET) spectrogram from THA/ESA, obtained during 1600 - 1630 UT, and X and Y components of the magnetic field from THA/FGM with the the IGRF components subtracted. The quasi-recurrent 2 - 3 min-long enhancements of the electron flux are observed during 8 min-long interval between 1610 and 1618 UT. They correspond to a set of 2 min-long variations of the magnetic field, embedded into about a 10 min-long increase, detected by THA/FGM between 1606 and 1618. This increase-then-decrease in dB_y may be interpreted as a signature of a field aligned current from the outward leg of the partial ring current.

3. Discussion

Multi-point observations by five THEMIS and TC-1 spacecraft during a substorm enabled the first through examination of the dynamics of ion and electron distributions in the transition region between the dusk-side equatorial plasma sheet and the inner magnetosphere within time scales of 2 - 3 hours and about 10 minutes.

On the hours time scale, the observations show inward/outward motion of the electron plasma sheet boundary during the AE increase/decrease. The population of ions with energy 5 - 50 keV with the distinctive nose-like dispersion appears during AE increase. The phase space density of these ions decreased with the decrease of the AE index, although the potential difference across the polar cap, on average, was stable.

Electrons with energies of 5 - 10 keV penetrated to the radial distance $R \approx 6\,\mathrm{R}_E$ and to the magnetic field $B \approx 130$ nT during the substorm with AE varying in the range 250 - 600 (interval II). Tracing 5 keV electrons from the positions listed in Table 1 back in time to in the dipole magnetic field and the global electric field in Volland-Stern (VS) form with the actual K_p [e.g., *Angelopoulos et al.*, 2002], we found their initial energy in the dusk-side plasma sheet at $R =$-12 R_E to be of 1.0 - 1.2 keV.

Electrons with energies of 0.5 - 1 keV may penetrate up to $R \approx 4\,\mathrm{R}_E$ and to $B \approx 460$ nT. It is questionable whether these electrons are on drift trajectories, mapped to the plasma sheet, or on closed drift shells. Tracing 1 keV electrons from the positions listed in Table 1 back in time, we found them trapped on closed drift trajectories. They persisted during about 5 hours. This population disappeared when the substorm decays.

Interpreting the $\sim$5 keV electron flux cut-off as the closest approach of the drifting plasma sheet electrons, experiencing gradient drift (co-rotation drift is neglected), we may roughly estimate the electric field variability using the equation for a position of the zero-flow point: $r_0 = [3\mu B_0 \mathrm{R}_E^3/|q|E]^{1/4}$, where B_0 is the dipole magnetic field at R=1 R_E at the equator, and E is the electric field. Using the data for 5 keV electrons from Table 1, we found that E increased by a factor of 1.4 between 1210 and 1549 UT, and decreased by a factor of 0.7 between 1604 and 1801 UT.

Ions with energies of about 10 keV penetrated to $R \approx 4\,\mathrm{R}_E$ and $B \approx 650$ nT during the substorm. Back-time tracing of the 10 keV ions from the positions listed in Table 2 gives their energies at R=12 R$_E$ in the pre-midnight sector of about 0.5 keV. These test particles need with 5 - 7 hours to travel from geostationary orbit to R=4 R$_E$ (see Table 2) in the dipole magnetic and the time-dependent VS electric fields with K_p varying between 2 and 3.5. On the other hand, the dynamics of the PS-like ion population in time scale of 1-3 hours was observed. Thus, although this model adequately reproduce the nose-like dispersion, it is inadequate to describe the dynamics. Estimation of the electric field variability using the equation for a position of the zero-flow point and the data listed in Table 2 yields an increase in a factor of 1.2 between 1335 and 1652 UT and a decrease in a factor of 0.9 between 1652 and 1927 UT.

On a smaller time scale, quasi-recurrent activations of the electron flux at energies 0.5 - 5 keV with the characteristic time of 1 - 3 min were detected during about 10 minutes-long interval at 5< R <6 R$_E$. These activations may result from acting of a transient local electric field generation. The characteristic time of the activations is consistent with the typical time scale of the fast flow bursts in the magnetotail [e.g., *Schödel et al.*, 2001] and dipolarisations, observed in the plasma sheet horn [*Apatenkov et al.*, 2007]. Thus the localized electric field due to the dipolarization following the flow burst may lead the observed electron flux enhancements.

Acknowledgments. We acknowledge NASA contract NAS5-02099, U. Auster and W. Magnes for the use of FGM data provided under the lead of the TU Braunschweig and with financial support through the German Ministry for Economy and Technology and the German Center for Aviation and Space (DLR) under contract 50 OC 0302; R. P. Lin, C. W. Carlson for use of SST and ESA data, E. Penou and A. Prentice for help with software and edition. We thank SuperDARN PI for the data available on the archive at JHAPL. The ACE WIND data are available on CDAWeb. We thank WDC for Geomagnetism, Kyoto for providing AE and Kp indices.

References

Angelopoulos, V. (2008), The THEMIS mission, *Space Sci. Rev*, *13x*, submitted.

Angelopoulos, V., M. Temerin, I. Roth, F. S. Mozer, D. Weimer, and M. R. Hairston (2002), Testing global storm-time electric field models using particle spectra on multiple spacecraft, *J. Geophys. Res.*, *107*, 1194, doi:10.1029/2001JA900174.

Angelopoulos, V., et al. (2008), First results from the THEMIS mission, *Space Sci. Rev*, *13x*, submitted.

Apatenkov, S. V., et al. (2007), Multi-spacecraft observation of plasma dipolarization/injection in the inner magnetosphere, *Ann. Geophys.*, *25*, 801–814.

Auster, H. U., et al. (2008), The THEMIS fluxgate magnetometer, *Space Sci. Rev.*, *xx*, submitted.

Buzulukova, N. Y., R. A. Kovrazhkin, A. L. Glazunov, J.-A. Sauvaud, N. Y. Ganushkina, and T. I. Pulkkinen (2003), Stationary nose structures of protons in the inner magnetosphere: Observations by the ION instrument onboard the Interball-2 satellite and modeling, *Cosmic Research*, *41*, 3–12.

Carr, C., et al. (2005), The double star magnetic field investigation: instrument design, performance and highlights of the first year's observations, *Ann. Geophys.*, *23*, 2713–2732.

Dandouras, I., J. Cao, and C. Vallat (2008), Energetic ion dynamics of the inner magnetosphere revealed in coordinated Cluster - Double Star observations, *J. Geophys. Res.*, *XX*, submitted.

Ejiri, M., R. A. Hoffman, and P. H. Smith (1980), Energetic particle penetrations into the inner magnetosphere, *J. Geophys. Res.*, *85*, 653–663.

Friedel, R. H. W., H. Korth, M. G. Henderson, M. F. Thomsen, and J. D. Scudder (2001), Plasma sheet access to the inner magnetosphere, *J. Geophys. Res.*, *106*, 5845–5858.

Ganushkina, N. Y., T. I. Pulkkinen, V. F. Bashkirov, D. N. Baker, and X. Li (2001), Formation of intense nose structures, *Geophys. Res. Lett*, *28*, 491–494.

Ganushkina, N. Y., et al. (2000), Entry of plasma sheet particles into the inner magnetosphere as observed by Polar/CAMMICE, *J. Geophys. Res.*, *105*, 25,205–25,220.

Kerns, K. J., D. A. Hardy, and M. S. Gussenhoven (1994), Modeling of convection boundaries seen by crres in 120-ev to 28-kev particles, *J. Geophys. Res.*, *99*, 2403–2414.

Larson, D., A. Angelopoulos, and J. P. McFadden (2008), THEMIS sst instrument, *Space Sci. Rev.*, *XX*, submitted.

Li, X., D. N. Baker, M. Temerin, G. D. Reeves, and R. D. Belian (1998), Simulation of dispersionless injections and drift echoes of energetic electrons associated with substorms, *Geophys. Res. Lett.*, *25*, 3763–3766.

McFadden, J. P., C. W. Carlson, D. Larson, V. Angelopolos, M. Ludlam, R. Abiad, and B. Elliot (2008), The THEMIS ESA plasma instrument and in-flight calibration, *Space Sci. Rev.*, *XX*, submitted.

Rème, H., et al. (2005), The hia instrument on board the tan ce 1 double star near-equatorial spacecraft and its first results, *Ann. Geophys.*, *23*, 2757–2774.

Schödel, R., W. Baumjohann, R. Nakamura, V. A. Sergeev, and T. Mukai (2001), Rapid flux transport in the central plasma sheet, *J. Geophys. Res.*, *106*, 301–313.

Sergeev, V. A., M. A. Shukhtina, R. Rasinkangas, A. Korth, G. D. Reeves, H. J. Singer, M. F. Thomsen, and L. I. Vagina (1998), Event study of deep energetic particle injections during substorm, *J. Geophys. Res*, *103*, 9217–9234.

Vallat, C., et al. (2007), Ion multi-nose structures observed by cluster in the inner magnetosphere, *Ann. Geophys.*, *25*, 171–190.

Wang, C.-P., L. R. Lyons, M. W. Chen, and F. R. Toffoletto (2004), Modeling the transition of the inner plasma sheet from weak to enhanced convection, *J. Geophys. Res.*, *109*, 12202, doi:10.1029/2004JA010591.

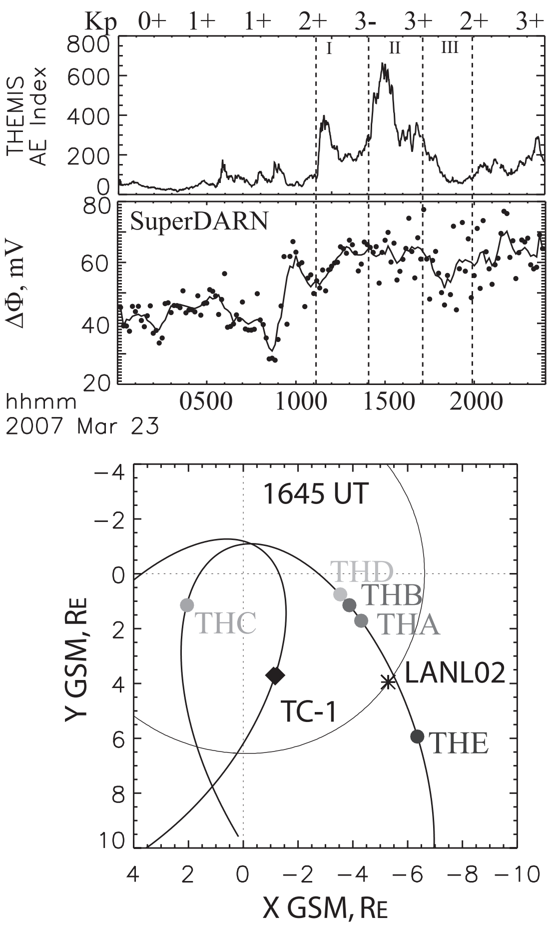

Figure 1. THEMIS pseudo AE index and the potential drop across the polar cap calculated from SuperDARN data during March 23, 2007 (upper panels, dots are 10 min averaged values, solid line shows the running average in 6-samples window). Vertical bars indicate times of the PS inner edge crossings. THEMIS, TC-1 and LANL02 spacecraft constellation at 1645 UT on March 23, 2007.

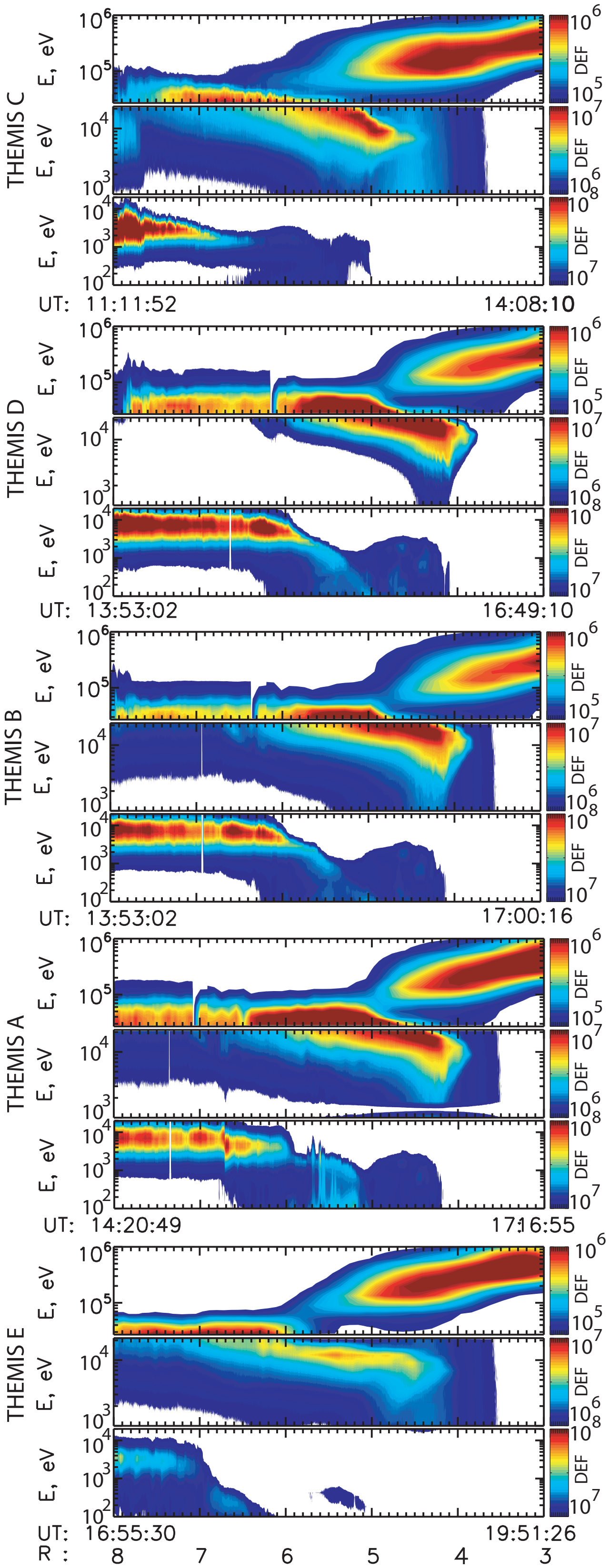

Figure 2. SST (upper panel) and ESA (mid panel) ion and ESA electron (bottom panel) spectrograms obtained by THEMIS spacecraft during inbound crossing of the inner edge of the plasma sheet on March 23, 2007

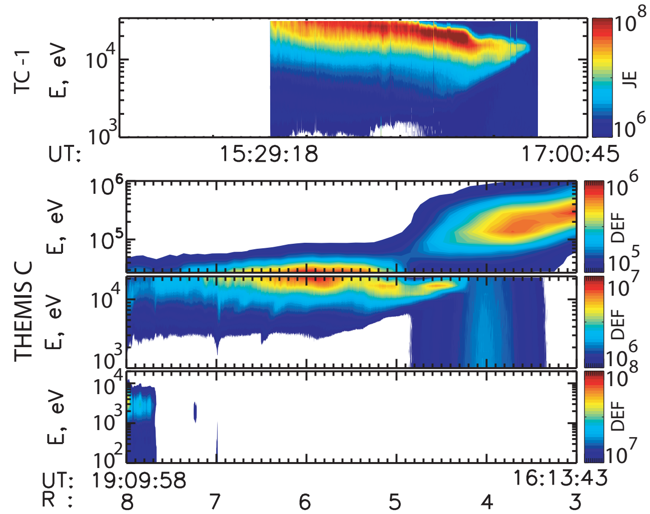

Figure 3. Spectrograms observed by TC-1 during inbound crossing at 20:00 LT and by THC during outbound crossing at 16:30 LT. Format is the same as in Figure 2.

Table 1. UT, LT, geocentric distance and GSM components of the magnetic field of the observed 5 and 1 keV electron flux cut-offs

SC	W, keV	UT, hh:mm	LT, hh:mm	R, R_E	B_x, B_y, B_z, nT
THC	5	12:10	21:41	7.5	-38.2, 32.6, 43.5
	1	13:05	22:15	5.6	-81.8, 50.7, 115.2
THD	5	15:42	22:12	6.2	-82.5, 55.4, 77.8
	1	16:30	23:00	4.2	-248.1, 108.4, 318.2
THB	5	15:49	22:08	6.0	-76.8, 53.8, 69.9
	1	16:44	23:04	4.1	-270.5, 111.4, 349.7
THA	5	16:04	22:07	6.3	-70.3, 51.5, 68.3
	1	16:58	23:00	4.3	-238.5, 104.9, 327.0
THE	5	18:01	21:44	7.5	-33.6, 31.4, 28.8
	1	18:19	21:54	7.0	-33.5, 25.7, 46.0
THC	5	18:34	17:16	7.7	9.2, -76.8, 34.8

Table 2. UT, LT, geocentric distance and GSM components of the magnetic field of the observed ion nose-like dispersions with maximum spectral density at ∼10 keV

SC	UT, hh:mm	LT, hh:mm	R, R$_E$	B_x, B_y, B_z, nT
THC	13:35	22:42	4.8	-170.4, 79.7, 233.1
THD	16:43	23:20	3.8	-398.9, 133.1, 490.5
TC1	16:51	19:39	3.6	-108.4, 495.0, 264.3
THB	16:52	23:16	3.9	-366.1, 125.5, 459.1
THA	17:07	23:14	4.0	-333.3, 119.3, 440.9
THE	19:27	22:52	4.5	-137.4, 61.3, 300.1
THC	16:35	15:54	4.3	-95.4, -289.2, 257.9

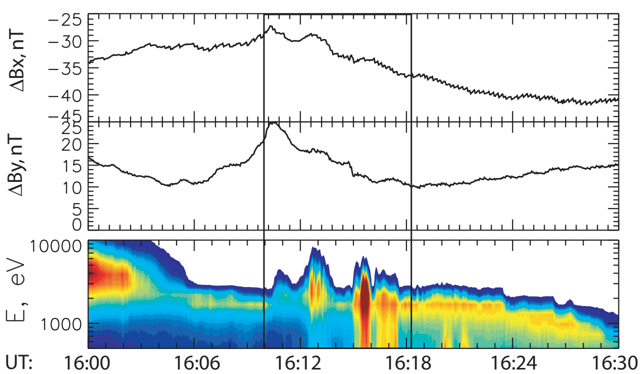

Figure 4. X and Y components of the magnetic field (IGRF magnetic field is subtracted) and the electron ET spectrum observed by THA during 1600 - 1630 UT.